Synergistic Incorporation of NaF and CsF PDT for High Efficiency Kesterite Solar Cells: Unveiling of Grain Interior and Grain Boundary Effects

Xiaohuan Chang[a†], Junjie Fu[a†], Dongxing Kou[a*], Wenhui Zhou[a], Zhengji Zhou[a], Shengjie Yuan[a], Yafang Qi[a], Zhi Zheng[b] and Sixin Wu[a*]

[a]*Key Lab for Special Functional Materials, Ministry of Education, National & Local Joint Engineering Research Center for High-Efficiency Display and Lighting Technology, School of Materials Science and Engineering, Collaborative Innovation Center of Nano Functional Materials and Applications, Henan University, Kaifeng 475004, China.*

[b]*Inst Surface Micro & Nano Mat, Coll Adv Mat & Energy, Key Lab Micronano Energy Storage & Convers Mat He, Xuchang University, Xuchang, Henan 461000, China.*

† Xiaohuan Chang and Junjie Fu contributed equally to this work.

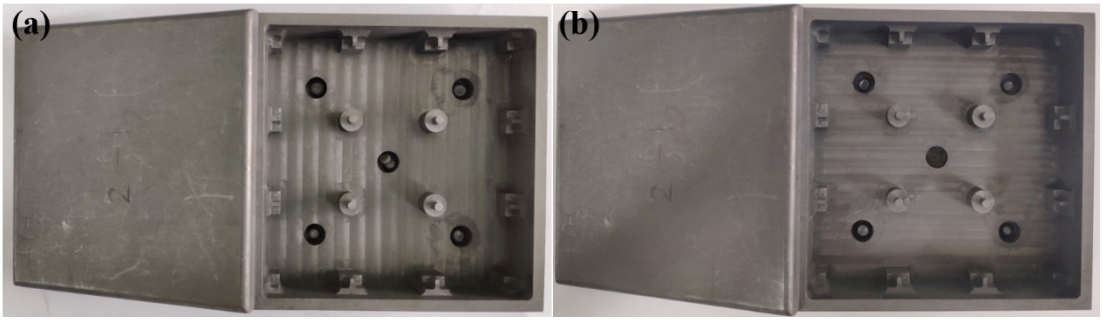

Fig. S1 Digital photographs of (a) 480 mg and (b) 320 mg selenium particles placed in the holes of graphite box for selenization and PDT treatment, respectively.

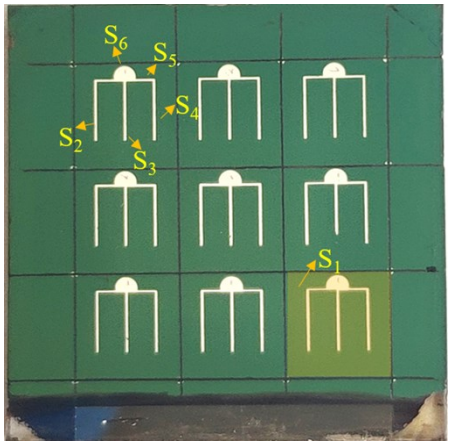

Fig. S2 Digital photograph of the fabricated CZTSSe solar cells. The unit is mm and the total area (S_1) of the solar cell is 0.2304 cm^2. After minus the silver grid area of S_2 (0.0029 cm^2), S_3 (0.0029 cm^2), S_4 (0.0029 cm^2), S_5 (0.0028 cm^2) and S_6 (0.0068 cm^2), the effective area is 0.2121 cm^2 for the fabricated device.

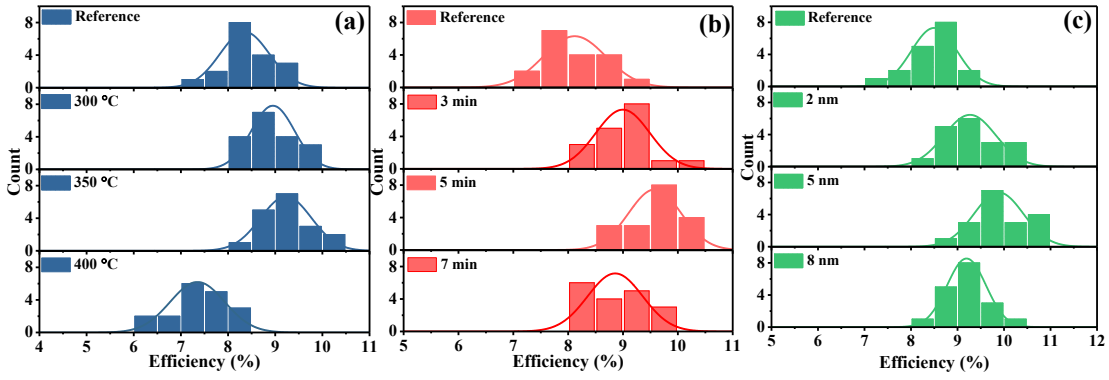

Fig. S3 The statistical distribution of cell efficiencies for CZTSSe cells with different LiF-PDT temperature (at 5 nm, 5 minutes), thickness (at 350 °C, 5 minutes) and the annealing time (at 350 °C, 5 nm.).

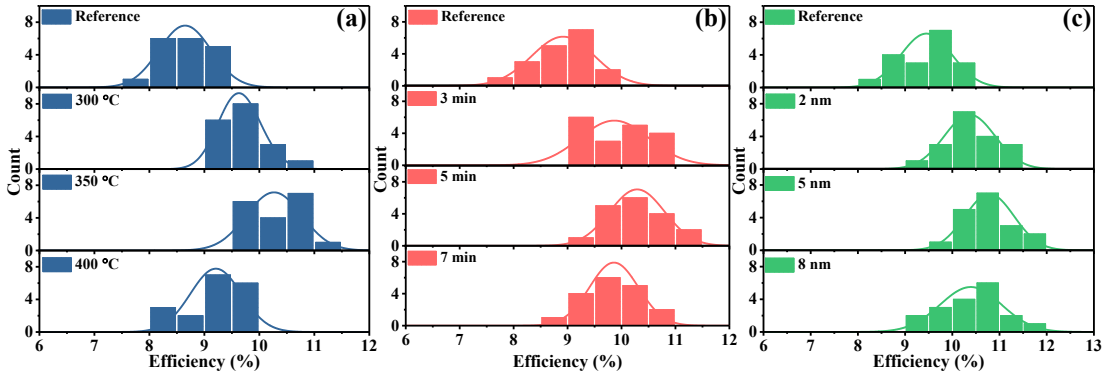

Fig. S4 The statistical distribution of cell efficiencies for CZTSSe cells with different NaF-PDT temperature (at 5 nm, 5 minutes), thickness (at 350 °C, 5 minutes) and the annealing time (at 350 °C, 5 nm.).

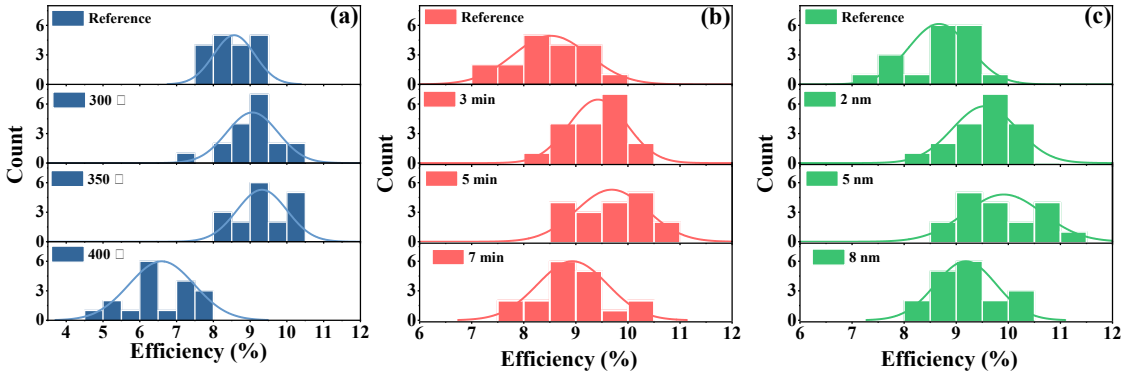

Fig. S5 The statistical distribution of cell efficiencies for CZTSSe cells with different KF-PDT temperature (at 5 nm, 5 minutes), thickness (at 350 °C, 5 minutes) and the annealing time (at 350 °C, 5 nm.).

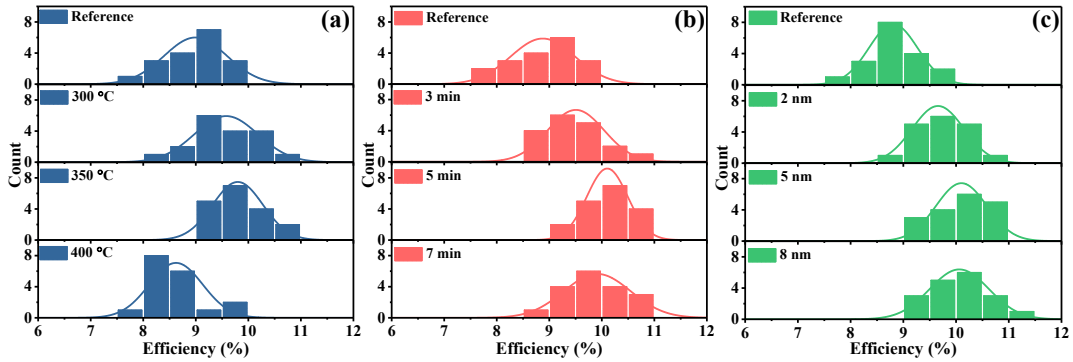

Fig. S6 The statistical distribution of cell efficiencies for CZTSSe cells with different RbF-PDT temperature (at 5 nm, 5 minutes), thickness (at 350 °C, 5 minutes) and the annealing time (at 350 °C, 5 nm.).

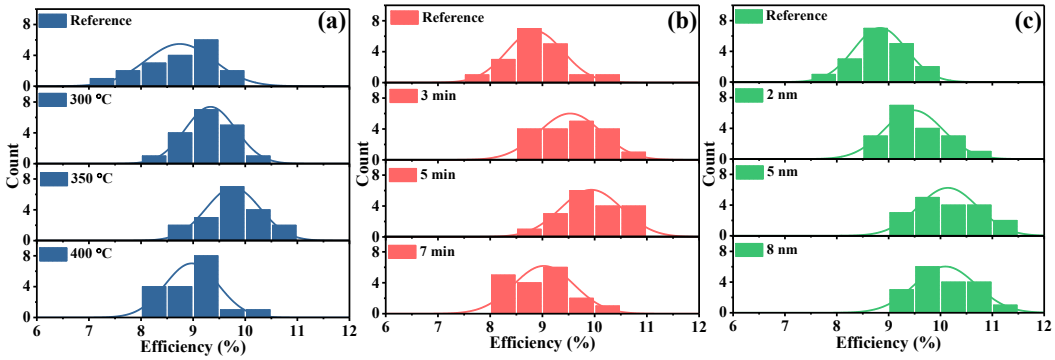

Fig. S7 The statistical distribution of cell efficiencies for CZTSSe cells with different CsF-PDT temperature (at 5 nm, 5 minutes), thickness (at 350 °C, 5 minutes) and the annealing time (at 350 °C, 5 nm.).

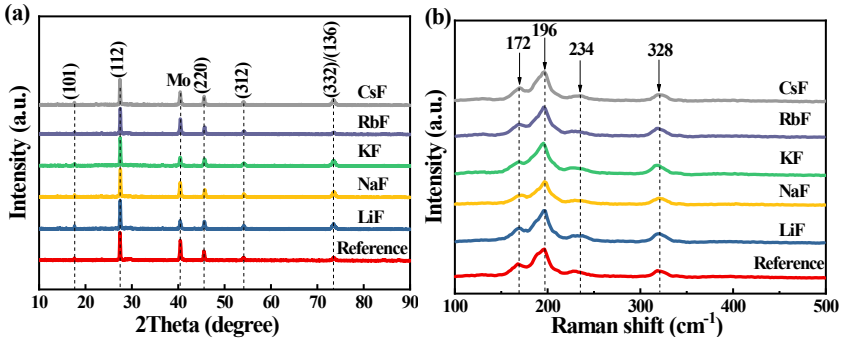

Fig. S8 (a) XRD patterns and (b) Raman spectrum of CZTSSe thin films after different AMs-PDT.

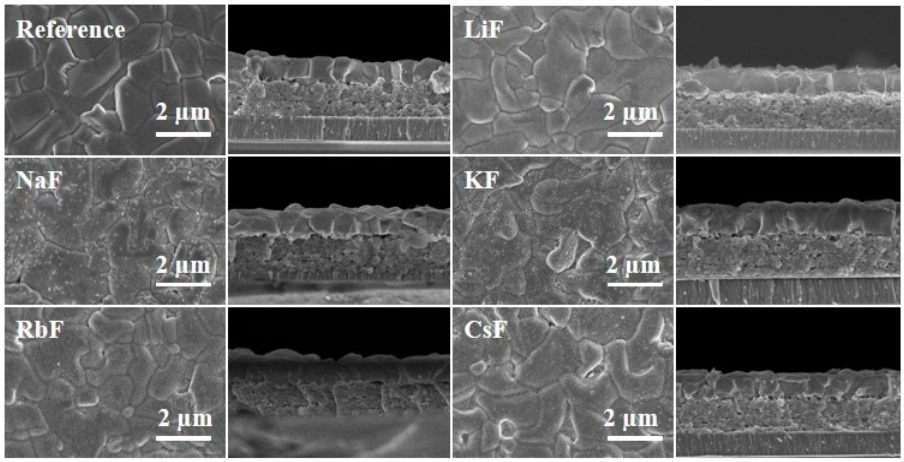

Fig. S9 Surface morphology and cross-sectional SEM images of CZTSSe thin films after different AMs-PDT.

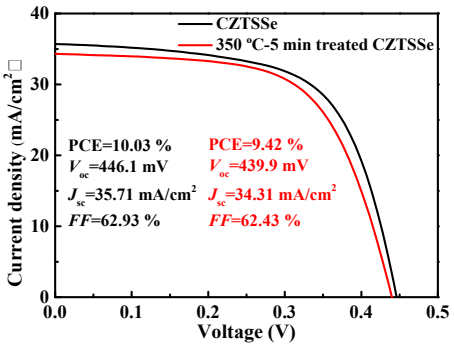

Fig. S10 *J-V* curves of CZTSSe solar cells before and after additional 350 °C, 5 min thermal treatment on selenized absorber.

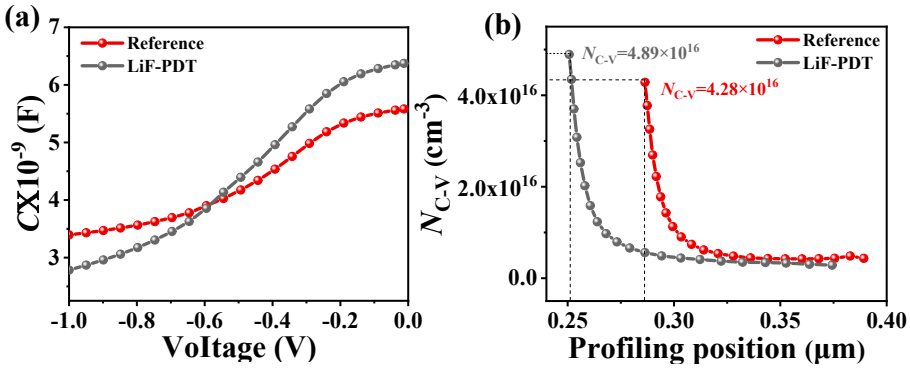

Fig. S11 (a) *C-V* curves and (b) extracted carrier concentration of Reference and LiF-PDT CZTSSe devices. These data are performed at room temperature with the bias range of -1 to 0 V.

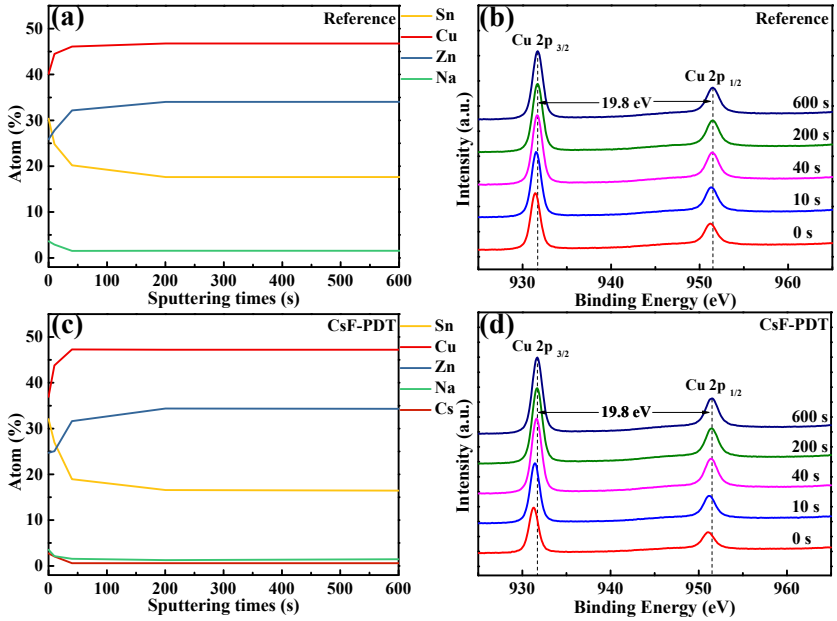

Fig. S12 XPS elemental depth profiles and XPS peak of Cu 2*p* obtained from (a)-(b) reference and (c)-(d) CsF-PDT CZTSSe films.

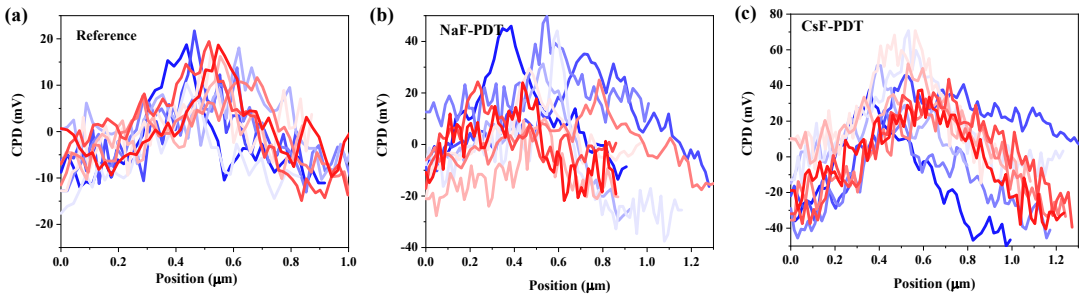

Fig. S13 The extracted CPD Line profiles around selected GBs for (a) Reference, (b) NaF-PDT, and (c) CsF-PDT CZTSSe thin films.

Table S1 The composition (mole percentage) of selenized CZTSSe absorber in our work derived from ICP measurement.

sample	Cu (%)	Zn (%)	Sn (%)	Se (%)	Cu/(Sn+Zn)	Zn/Sn
CZTSSe	26.48	17.84	16.56	39.12	0.77	1.08